

- Seismic Retrofit Measures for Highway Bridges. FHWA, Rept. FHWA-TS-216, Vol. 1, April 1979.
23. T. Iwasaki. Earthquake Resistant Design of Bridges in Japan. Ministry of Construction, Tokyo, Vol. 29, May 1973.
 24. M. Ohashi, E. Kuribayashi, T. Iwasaki, and K. Kawashima. An Overview of the State of Practices in Earthquake Resistant Design of Highway Bridges in Japan. Presented at Workshop on Research Needs of Seismic Problems Related to Bridges, San Diego, CA, Jan. 1979.
 25. N. Yamadera and Y. Oyama. Special Considerations and Requirements for Seismic Design of Bridges in Japan. Metropolitan Expressway Public Corp., Tokyo, n.d.
 26. I.C. Lin. Equivalent Seismic Design of Curved Box Girder Bridges. Department of Civil Engineering, Univ. of Maryland, College Park, M.S. thesis, April 1981.

Publication of this paper sponsored by Committee on Dynamics and Field Testing of Bridges.

Test to Failure of the Hannacroix Creek Bridge

DAVID B. BEAL

A 52-year-old reinforced concrete T-beam bridge was destructively tested to evaluate the consequences of concrete deterioration on load capacity. Instrumentation included measuring tension and compression rebar strain at midspan, end rotation, and midspan deflection. The single- and double-T test specimens were loaded symmetrically to produce a constant-moment region at midspan. The condition of the bridge was rated 2.5 on a scale from 1 (potentially hazardous) to 7 (new condition). The concrete deck was highly fractured throughout and the cement paste severely deteriorated locally. Efflorescence was common and leakage was evident. Tension rebars exposed by spalled concrete had lost 1-2 percent of their cross-sectional area. It is concluded that the deterioration noted has no significance with respect to the load-carrying capacity of the structure. Based on theoretical arguments, it is concluded that deterioration sufficient for substantial reduction in the capacity of a structure would be manifested in a local collapse and that overall failure of reinforced concrete T-beam bridges need not be a concern.

National bridge inspection standards require that highway bridges be inspected and rated for load-carrying capacity. For steel structures, the guidelines are straightforward and they can be rated without difficulty. Reinforced concrete bridges, by contrast, are not easily rated because the significance of deterioration may be unquantifiable. Because of this difficulty, in 1978 New York State initiated a research program to develop a low-cost field testing method for evaluating structural strength. This effort was abandoned when, at the load levels attainable, it was shown that bridges with sound and deteriorated concrete did not differ in behavior (1).

Because service-load tests could not show differences attributable to deterioration, a test to failure of a heavily deteriorated bridge was planned. It was believed that correlation of the results of such a test with the findings of a thorough pretest inspection and evaluation would give some insight into quantification of the effects of observable deterioration.

TEST STRUCTURE

The test structure is a reinforced concrete T-beam bridge constructed in 1930 that carries NY-32 over the Hannacroix Creek in Albany County. It consists of seven beams 39.5 in long and a 36-ft clear span between faces of the abutments. Nominal cross-section dimensions and reinforcement details for an interior beam are shown in Figure 1. In addition, a nonstructural 4-in concrete wearing surface and a 3-in asphalt wearing surface were removed before testing. The flexural reinforcement consists of

eight 1.25-in-square deformed bars that provide a nominal cross-section area of 12.5 in² for a reinforcement percentage of 2.25. Compression reinforcement is negligible. In the center 21 ft, 10 in, shear reinforcement spacing exceeds the limits set by current specifications (2, p. 78).

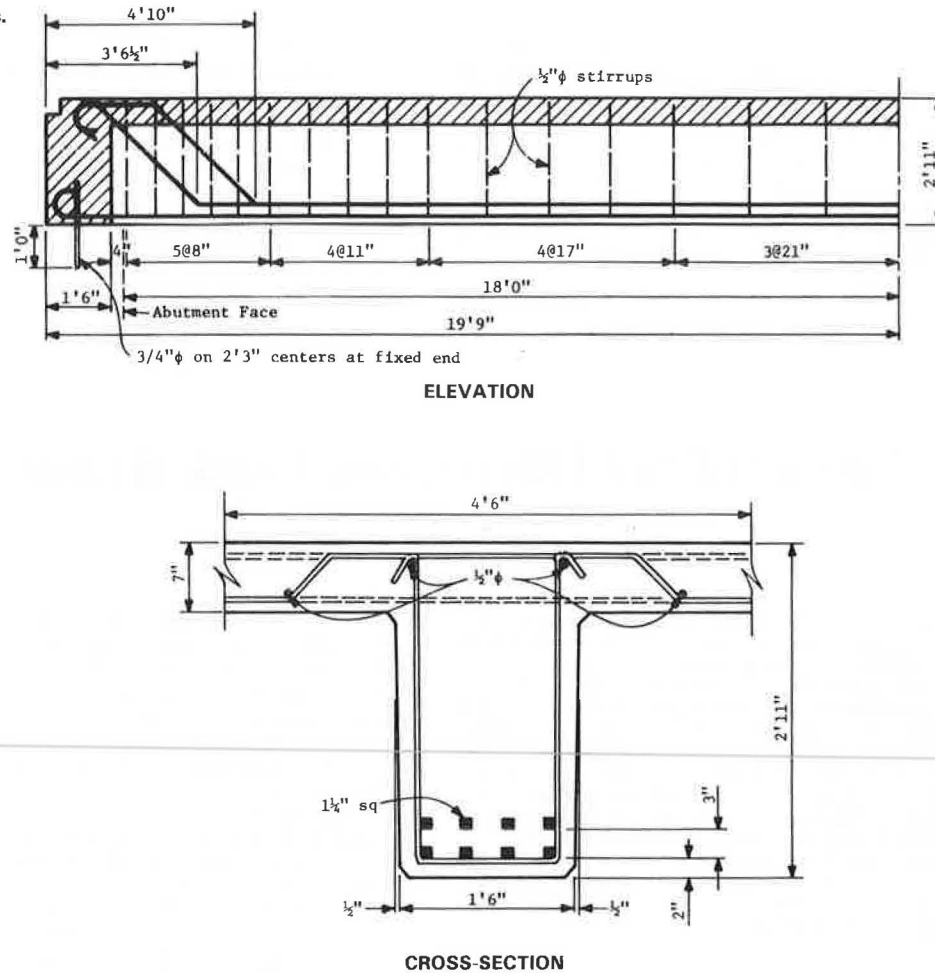
The expansion end bearings consist of steel plates separated by a layer of graphite grease. This detail makes no provision for end rotation. At the "fixed" ends, 0.75-in-diameter rods are embedded in the abutment and end diaphragm. The beam ends and diaphragm rest directly on the abutment, a detail that restrains translation and rotation.

Bridge condition at the time of testing was poor. The most recent inspection report rates the primary members at 2-3 on a scale from 1 (potentially hazardous) to 7 (new condition). Figure 2 shows a photo montage of the underside of the structure that, except for slight transverse parallax, reliably shows its condition. Spalled concrete areas exposing the tension rebars in the beam stems are evident. The exposed rebars are rusted but do not appear to have suffered more than 1-2 percent loss of cross-sectional area. Although it is not visible in Figure 2, the vertical faces of all beams exhibited extensive cracking, generally paralleling their axes. Efflorescence (the white areas in Figure 2) is common and leakage is evident.

Cores drilled through the deck showed it to be highly fractured throughout and that the cement paste was severely deteriorated locally. The disintegration of the 4-in concrete wearing surface may be linked to its relatively high absorption (3). Failure of the structural deck concrete is judged to have resulted from the freezing of water in pores of the cement paste, aggravated by the presence of chlorides in solution. Deterioration of the T-beam stems has resulted from the same causes, plus corrosion of the steel reinforcement. These mechanisms are facilitated by increased permeability, presumed to be related to absorption. Mean absorption of seven core segments taken from the structural deck was 5.6 percent. This value is greater than about 80 percent of values measured in cores from other New York bridge decks. The upper 1 in of structural deck was disintegrated and came off with the concrete wearing surface. Thus, the structure was tested with a 6-in slab (see Figure 3).

Sonic pulse-velocity measurements through the stems of beams 3, 4, and 6 yielded values of 1700-4400 ft/s. Although precise correlation of concrete

Figure 1. Nominal dimensions.



strength with pulse velocity has been found to be infeasible (1), such low values as these suggest concrete with low compressive strength. For comparison purposes, pulse velocities measured on 62 cylinders with compressive strengths ranging from 2000 to 5000 psi were never less than 12 500 ft/s (1).

Obtaining cores suitable for compression testing was difficult because of the extensive concrete deterioration. The mean of the two tests performed was 4200 psi and the range 1000 psi. Because of the noted disintegration of the deck and the low pulse-velocity values, this result is taken as indicating the unreliability of cylinder tests in predicting concrete strength in deteriorated structures.

Tension tests on 24 samples of the 1.25-in-square bars gave an average yield strength of 44 ksi. A single sample of the 0.5-in-diameter structural deck reinforcement had a yield strength of 46.5 ksi. Average loss of square bar cross section determined on a weight-per-unit-length basis was 2.1 percent from twenty-four 30-in samples and 2.8 percent from twenty-seven 2-in samples. Maximum loss of 6.6 percent occurred in a 2-in length; 3.2 percent loss was the maximum in a 30-in length. Loss was calculated from an assumed nominal area of 1.56 in². Although the structural deck steel was not randomly sampled, areas exposed during testing showed no corrosion. The chloride content of the structural deck, determined from drilled samples of concrete powder, was erratic. It averaged only 2.5 lb/yd³, and the maximum value was 2.8 lb/yd³. These relatively low values are probably the best explanation

of the minor rebar corrosion noted. Chemical analysis of the steel showed no alloying elements expected to increase corrosion resistance.

The structure was designed to carry a live load of 20-ton trucks. With working stresses of 20 000 psi for the grade 40 steel and 1650-psi concrete (3000-psi compressive strength was assumed) (4), the maximum permissible live-load bending moment is 48 percent larger than the design moment due to HS-20 trucks (2). By using a load-factor approach ($f_y = 40\ 000$ psi, $f'_c = 3000$ psi), the inventory rating determined for this structure is 1.76 HS-20 design loads. The operating rating for the bridge is 2.55 or 2.93 HS-20 design loads by working stress or load factor, respectively. None of these calculations accounts for the consequences of the noted deterioration.

With respect to shear, it has been noted that spacing of stirrups in the central portion of the beam is greater than current specifications permit (2). At the supports, however, the provided reinforcement is adequate for 1.32 HS-20 trucks or 1.08 HS-20 trucks for service-load design or load-factor design, respectively.

TEST PROCEDURES

Because of site conditions that prevented detouring of traffic, the structure could not be tested as a single unit. Three separate tests were performed. Two of these were on single-stem units with the associated structural slab, and the third was on a two-stem unit with the associated slab (Figure 3).

Figure 2. Underside of Hannacroix Creek bridge (beam numbers at right).

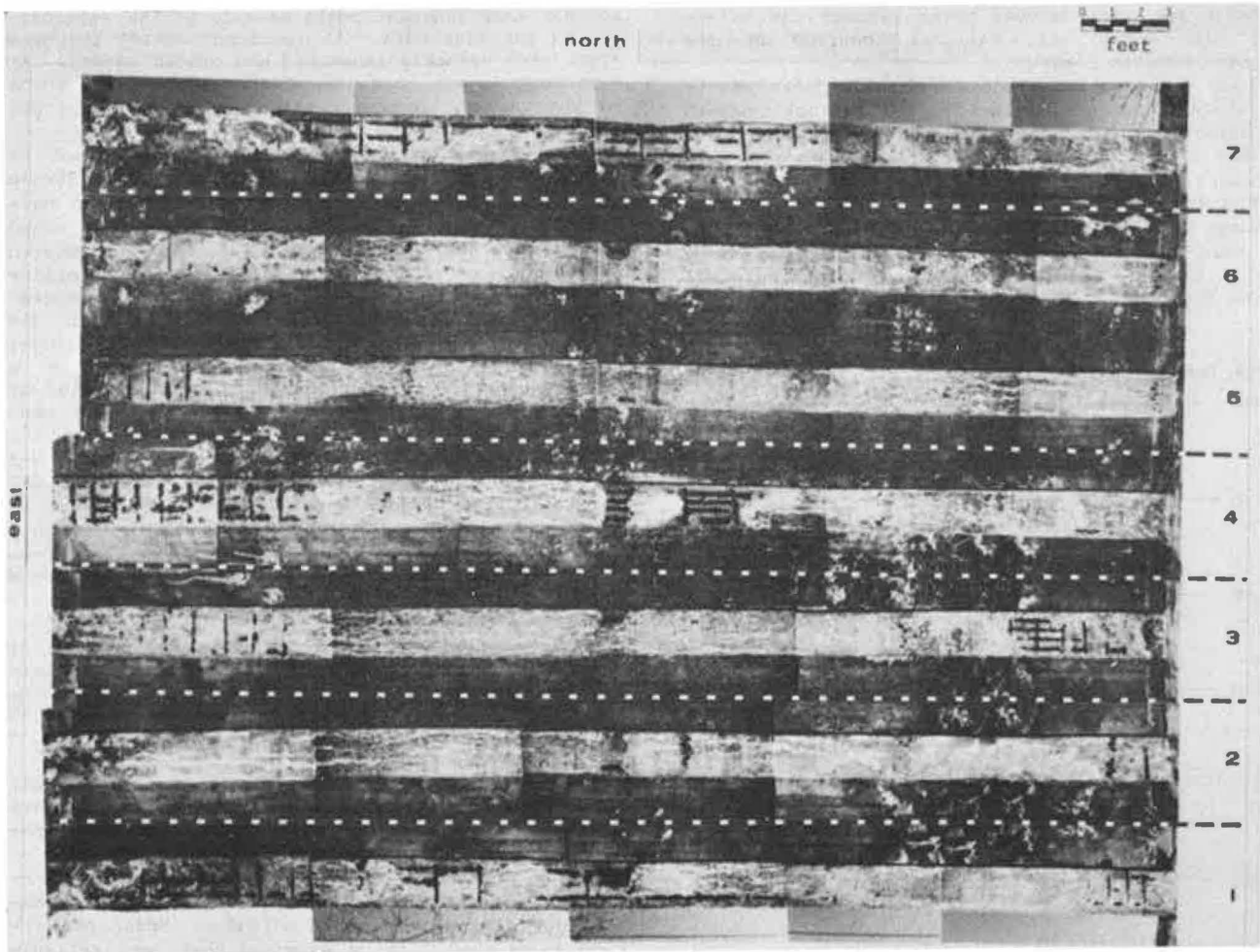
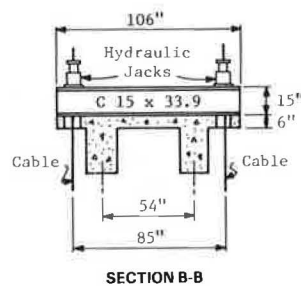
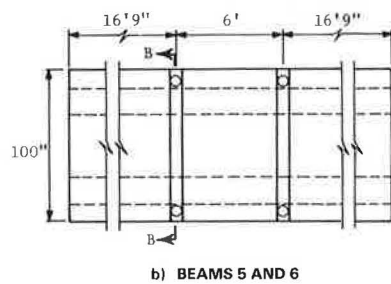
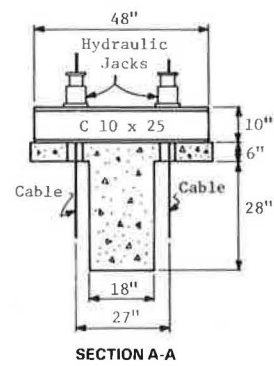
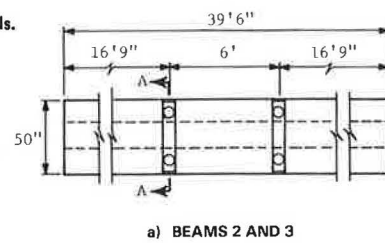


Figure 3. Test specimen details.



Locations of these units in the structure and their condition before testing can be seen in Figure 2. Although the cable access holes reduced the effective slab width, all failures occurred at the midpoint between loads.

Loads were applied through hydraulic jacks reacting against cables embedded in the bedrock beneath the structure. The load positions shown in Figure 3 provide a 6-ft constant-moment region. Loads were increased slowly from one load increment to the next without impact.

Loads were monitored through a pressure gage that had been calibrated with the hydraulic rams in a test machine. A manifold was used to distribute oil to the four rams. The loading scheme consisted of a

series of loading-unloading cycles up to failure. This scheme provided partial replication of the test so that some judgment could be made on the reliability of the test data. At low load levels, the beam stems were visually inspected and cracks marked. At high load levels, because of the considerable force in the cables, it was considered imprudent to get close to the beams.

Instrumentation was provided for measurement of strain, displacement, and end rotation. Strain gages were bonded to each of the four tension bars in the bottom row (Figure 1) and to a 0.5-in round compression bar in the slab. Two sections located symmetrically 1 ft on either side of the centerline were instrumented. The 0.25-in-long, self-temperature-compensating gages had a resistance of 350 Ω . They provided one arm of a Wheatstone bridge, completed at the instrumentation located in a trailer near the test structure. Leads consisted of 250-ft-long, four-conductor no. 22 wire with conductors paired under separate foil shields.

Displacements were measured with a Wilde N-3 level capable of measurements to the nearest 0.001 in. Calibrated targets were placed on the bridge at the supports and at midspan. In addition, targets were placed symmetrically at points 6 and 12 ft from the supports. These latter targets were monitored at selected loads only. A fixed benchmark was positioned off the structure.

End rotation was monitored from measurement of the relative displacement of two points on a rigid bar attached to the girder ends with respect to the abutment face. The rotation measurement caused much difficulty, and the theoretical accuracy of 3×10^{-6} rad was not achieved.

The accuracy of field measurements is difficult to determine because of general inability to perform replicates. The assumed precisions of $10 \mu\epsilon$ for strain, 0.01 in for deflection, and 0.0001 rad for rotation are based on experience with similar measurements and examination of the internal consistency of the data obtained here. Under no circumstances should it be expected that more reliable values have been obtained.

TEST RESULTS AND DISCUSSION

Analysis of the rebar strain measurements showed no trends with respect to longitudinal or transverse position of the bar in a beam cross section. Thus, despite the physical difference between rotational restraint capabilities of the fixed and expansion ends (Figure 1), the raw strain data were insufficient to demonstrate a difference. Except at high strains, the average of all eight bars was taken as

Figure 4. Tension strain versus load for all beams.

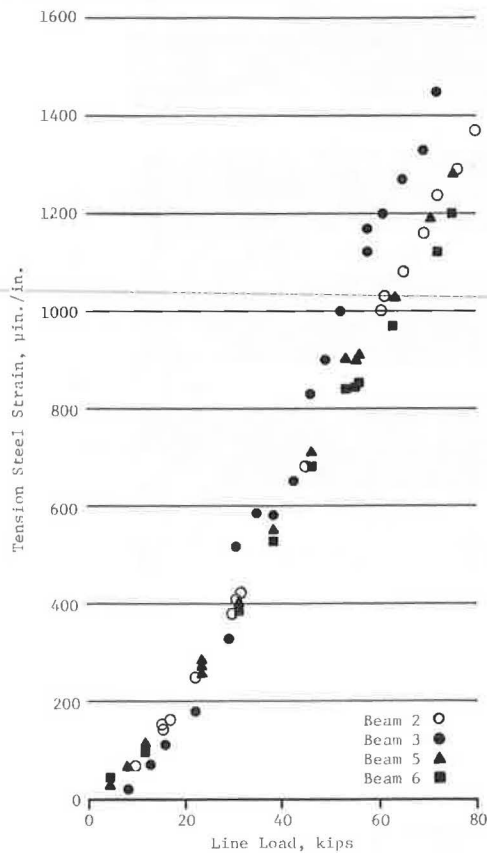
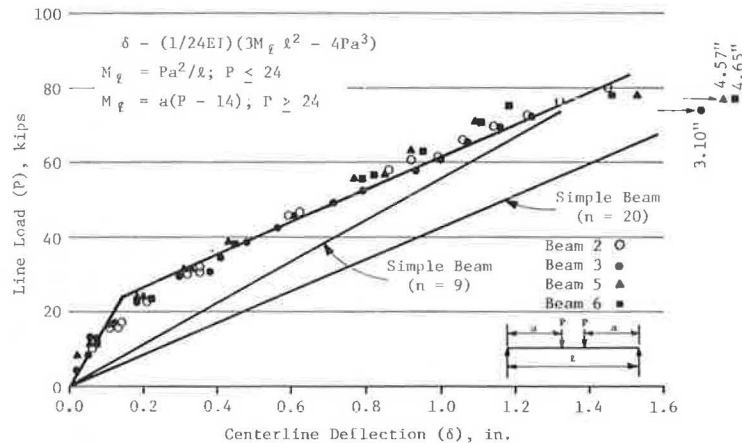


Figure 5. Load versus deflection for all beams.



the best estimate of rebar strain. Additional details of the data analysis procedures can be found in the full report (11).

Figure 4 gives tension strain versus load for all beams. Only strains at peak loads are plotted. Data

from loading-unloading cycles have been deleted for clarity. Despite variation in the magnitude of residual strains, it should be noted that the four beams behaved in a similar manner and that the relation between load and tension strain is largely linear. Extreme values are represented by beams 3 and 6, beam 3 giving the largest strain values.

Figure 5 presents a composite drawing that shows load versus centerline deflection for peak loads only. This relation is also similar to that shown for tension strains and indicates linear behavior for loads greater than 20 kips and less than 80 kips. In addition, differences between beams are less than for tension strains, an expected result since deflection represents an averaging of strain along that full length of the beam.

Load versus end rotation is shown in Figure 6. This measurement proved to be unreliable. Data were lost at the fixed end of beam 2 and the expansion end of beams 5 and 6. Some insight into the behavior of the structure can be gained, however, from the data obtained. First, it should be noted that rotations were zero in all cases for loads less than about 18 kips. For beam 3, the load needed to cause first rotation was substantially larger. Once rotation occurred, however, the relation between load and end rotation was largely linear. These data imply that both ends of the beam were supplying some moment restraint. The differing slopes of the lines for beams 3 and 2 indicate that beam 3 is slightly more flexible than beam 2 after release occurs. The flexibility for both ends of beam 3 is approximately equal, although the release load is larger at the fixed end of this beam.

Centerline bending moments for peak loads are plotted versus line load in Figure 7. The values for beams 2, 5, and 6 define a bilinear relation. Because the rotation measurements showed zero rotation or moment fixity at low loads and the strain data indicated a constant value of flexural stiffness (11), the first portion of a bilinear load versus moment relation is taken as that for a fixed-ended beam. This relation satisfactorily fits the data for moments less than 2000 kip-in. For comparison purposes, a line representing the simple-beam relation is also shown and clearly does not fit the data. The plotted relation was calculated for a span length of 37 ft.

The upper linear portion of the moment-load relation is taken with a slope equal to the shear span (a in Figure 7), the simple-beam value. Again, this

Figure 6. Load versus end rotation.

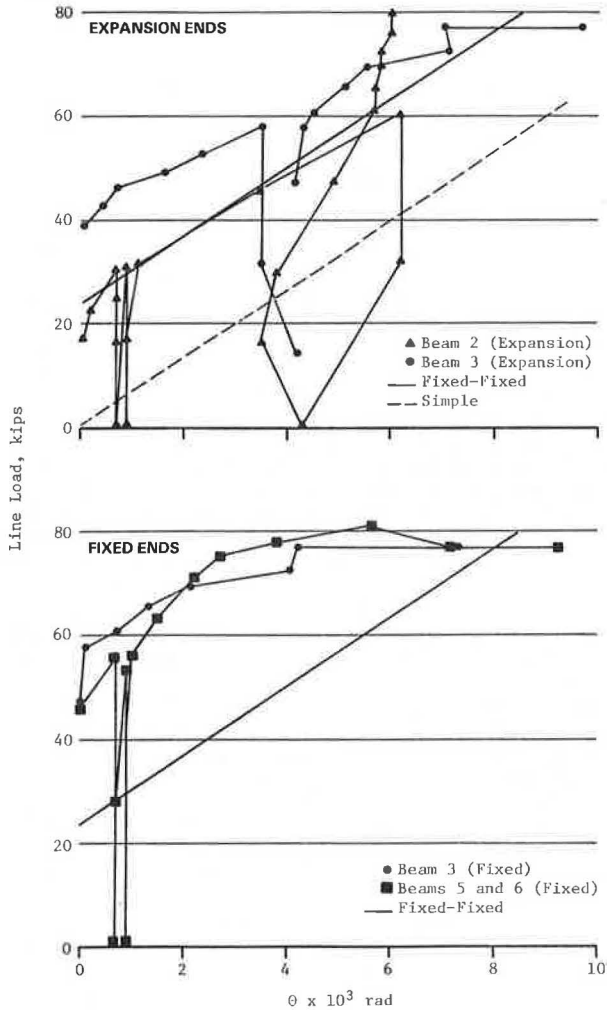


Figure 7. Load versus bending moment.

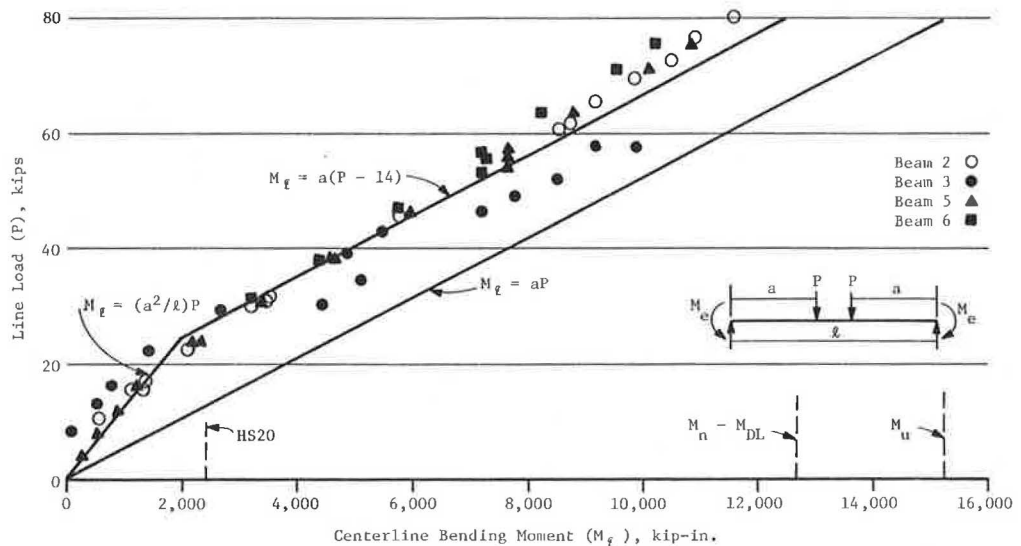
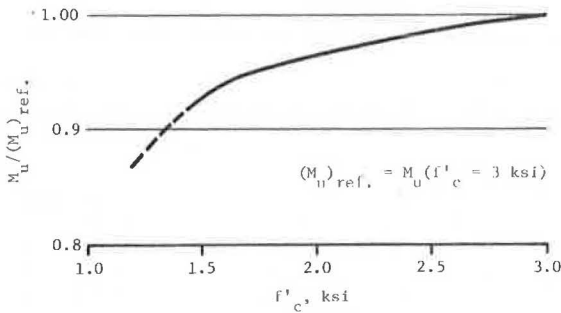


Figure 8. Influence of concrete strength on bending resistance.



is suggested by the rotation data, which indicate a constant value of end restraint after release. The intersection point for the two linear segments was selected by fitting the "best line" with the simple-beam slope.

By using similar reasoning, a relation between bilinear load and centerline displacement was derived (Figure 5). The flexural stiffness is taken as 150×10^6 kip-in², as found from the strain data (11). Comparisons between calculated and measured deflections are good. Of particular note is the correspondence between the theoretical relation and beam 3 data. This result suggests that the beam 3 strain data are defective.

The slope of the relation between load and end rotation implied by the centerline moment analysis compares reasonably well with the experimental results (Figure 6). Except for the beam 2 expansion end, however, the 24-kip end-restraint release load is substantially less than the experimental value.

It is important to emphasize that no part of the preceding analysis is of particular significance with respect to the general load-rating problem. The analysis was performed to demonstrate the consistency (or lack of consistency) between the various forms of collected data and to permit estimation of the elastic modulus. From the results presented, it can be concluded that the measured values reliably represent the true behavior of the test specimens.

The only unexplained aspect of beam behavior is the end restraint indicated by all three measurements. The break point of the bilinear moment-load relation implies a maximum end moment of 2520 kip-in. It is difficult to believe that this magnitude of moment could be developed at the expansion end of the beams. Even at the fixed end with the 0.75-inch diameter dowels, the level of moment is unrealistically large. The ultimate moment of this detail (taking account of the moment enhancement due to the beam reaction) is only 660 kip-in. Nevertheless, the existence of large-magnitude end moments cannot be disputed in view of the measurements obtained.

The large difference between the modular ratio found here and the values used in design should be placed in perspective. First, the consequence of varying the modular ratio from 20 to 9 [a nominal value often assumed in design (2)] is to increase the ratio of bending moment to rebar strain by only 5 percent. Because of this small variation, it should be clear that the analysis used to obtain the experimental value is extremely sensitive to small variations in measured strain. Thus, the reported value of 20 cannot be claimed to be exact. Second, the variation in flexural stiffness over the same range is 30 percent, and this magnitude could easily be detected in the data. Comparison of measured and calculated deflections (Figure 5) demonstrates that the correct stiffness is predicted well by the modular ratio of 20 and suggests that this value is

more representative of the actual stiffness of the structure than the nominal value of 9. Third, it is wrong to calculate a cylinder strength by using the modular ratio and the empirical relation devised by Pauw (7), since the inverse of this equation is not a "best fit". Thus, the only significance of the value of 20 is as a measure of stiffness and not of strength.

APPLICATION TO LOAD RATING

It is not possible or prudent to extrapolate the findings from a single test to a general set of load-rating rules. It would clearly be inappropriate, for example, to propose that a certain level of end-moment restraint be assumed for all structures because of its existence in this structure. The same is true with respect to the findings on rebar yield strength. In addition, the data obtained are for overall collapse and cannot be used to predict local failures. What, then, can be taken from the present tests and applied to the load-rating problem?

The data available can be used to estimate the reduction in load capacity, if any, from capacities predicted analytically. Unfortunately, the centerline moment at failure is unknown, but it must lie between the boundaries defined by the bilinear relation shown in Figure 7 and the relation for a simple beam. These relations establish limits for the failure moment of 1010 and 1230 kip-ft. Alternatively, the largest moment derived from the data was at the limits of elastic behavior. For this section, the theoretical ratio of maximum elastic moment to ultimate moment is 0.86. Using this value and the maximum experimental moment of 960 kip-ft gives an estimated failure moment of 1140 kip-ft (11). This value is at about the midpoint of the range defined earlier.

The theoretical failure moment determined by using actual steel yield and cross-section dimensions and accounting for the dead-load moment is 1120 kip-ft. Thus, the theoretical failure moment is at the midpoint of the possible range of actual failure moments. Because of this result, it is concluded that no evidence exists to suggest that moment resistance of the section has been decreased by either apparent concrete deterioration, loss of rebar cross section, or loss of rebar cover.

This conclusion, which is specific for the structure tested, can be generalized to apply to the complete family of concrete T-beam bridges. This is possible because the conclusion drawn from this test can be shown analytically. For example, the variation in ultimate moment resistance as a function of concrete strength is shown for the test bridge in Figure 8. Nominal section dimensions and 44-ksi yield-point reinforcement have been assumed in these calculations. From this figure, it can be seen that a 50 percent reduction in concrete strength (from 3 to 1.5 ksi) results in only a 7.5 percent reduction in ultimate bending resistance. It is assumed that local failures would occur for strengths less than 1500 psi, and thus this value is taken as a practical lower limit for rating. A similar analysis shows that a 50 percent loss of slab thickness decreases the flexural capacity of the beam by only 12 percent. It should be noted that the ability of the slab to support wheel loads would be severely reduced with a thickness loss of this magnitude and that deck failure would occur before beam failure (8).

The relation between flexural strength and tension reinforcement area is nearly linear. In practice, however, large losses in rebar area are unlikely. In this structure, the tension reinforcement is distributed in two layers and only the

exposed lower layer had any loss. Nevertheless, it may be prudent to require that inspectors record a visual estimate of cross-section loss. It is not unreasonable to assume that beams with cover intact have experienced no important loss of tension reinforcement area.

In general, it is not possible to evaluate shear capacity directly by means other than failure testing. The beams tested in this work did not fail in shear despite being subjected to loads three times larger than the maximum design value over all but the center 6 ft of the span. The shear cracks, which opened just outside the center region of zero shear (constant moment), are a consequence of the wide stirrup spacing near the centerline of this bridge. At this location the applied shear was 10 times larger than the design value, which suggests that this wide spacing is not a critical defect. In addition, the lack of bond failure is taken as evidence that loss of rebar cover is not detrimental to strength. It has been shown by others (9) that loss of cover alone has little short-term effect on the behavior and strength of reinforced concrete beams.

The test beam failed by crushing of the concrete, an apparent consequence of reduced compressive strength. This crushing failure reduced beam ductility as measured by ultimate deflection. The theoretical ultimate deflection was estimated at about 12 in (10), but the actual values ranged from 3.1 to 4.6 in. Although the actual deflections at failure are substantially less than the theoretical values, they are roughly three times larger than the elastic values predicted by the first equation in Figure 5. In addition, the lower rebars yielded before failure. Thus, the apparent loss of ductility does not compromise the load rating of the structure.

Based on the conclusion that normal forms of deterioration are not severely detrimental to the load capacity of reinforced concrete T-beam bridges, the following load-rating strategy can be used:

1. Assemble as nearly complete a set of standard sheets as possible.
2. Demonstrate that existing bridges for which no plans are available are from the standard sheets. This can be done by means of a random survey of such bridges where a set of key measurements is made. For New York State standard sheets, for example, the clear span, stem depth, and girder spacing uniquely identify the structure. Bridges with combinations of these values that are inconsistent with the standard sheets cannot be rated by this technique.
3. Analyze standard bridges for load-carrying capacity. Reduction factors can be devised for estimated losses of concrete strength, structural deck thickness, and rebar cross sections if feasible inspection procedures can be derived. Alternatively, assuming 2000-psi concrete in analysis will reduce the possible strength reduction to less than 4 percent, a tolerable value, and the minor consequences of other forms of loss can be ignored. Inspectors should be alerted to note large areas of rusted reinforcement and to estimate the area loss. In these instances, individual calculations are required. It is likely that shear capacity may control the rating in many cases, especially for short bridges such as the one tested.

CONCLUSIONS

The structure tested showed no reductions from nominal load capacity despite its apparently heavily deteriorated condition. The unexpected compression failure occurred after rebar yield and at suffi-

ciently large displacements to give ample warning of impending collapse. It has been demonstrated that the insensitivity of the test structure to deterioration is predictable analytically. It is concluded that deterioration sufficient for substantial reduction of the capacity of the structure would be manifested in a local collapse and that overall failure need not be a concern. Finally, a strategy for load rating is outlined that is founded on the conclusions drawn in this paper and the belief that older structures were constructed with care that reliably duplicated the design.

ACKNOWLEDGMENT

Robert J. Kissane assisted in planning the testing described in this paper and was responsible for supervising the field work. Edward W. Bikowitz, Everett W. Dillon, Frank P. Pezze, and Scott P. Ross installed instrumentation and assisted in monitoring the structural response to load. This research was conducted in cooperation with the Federal Highway Administration, U.S. Department of Transportation.

REFERENCES

1. R.J. Kissane, D.B. Beal, and J.A. Sanford. Load Rating of Short-Span Highway Bridges. Engineering Research and Development Bureau, New York State Department of Transportation, Albany, Res. Rept. 79, May 1980.
2. Standard Specification for Highway Bridges: Section 1.5.10(C)--Spacing Limits for Shear Reinforcement. Structures Design and Construction Subdivision, New York State Department of Transportation, Albany, Jan. 1982.
3. D.B. Beal and W.P. Chamberlin. Effects of Concrete Deterioration on Bridge Response. TRB, Transportation Research Record 853, 1982, pp. 43-48.
4. Manual for Maintenance Inspection of Bridges. AASHTO, Washington, DC, 1974.
5. N.L. Johnson and F.C. Leone. Statistics and Experimental Design. Wiley, New York, 1964, Vol. 1, pp. 242-244.
6. E. Hognestad, N.W. Hanson, and D. McHenry. Concrete Stress Distribution in Ultimate Strength Design. Journal of the American Concrete Institute, Dec. 1955, pp. 455-480.
7. A. Pauw. Static Modulus of Elasticity of Concrete as Affected by Density. Journal of the American Concrete Institute, Dec. 1960, pp. 679-687.
8. D.B. Beal. Strength of Concrete Bridge Decks. Engineering Research and Development Bureau, New York State Department of Transportation, Albany, Res. Rept. 89, July 1981.
9. I. Minkarah and B.L. Ringo. Behavior and Repair of Deterioration Reinforced Concrete Beams. TRB, Transportation Research Record 821, 1981, pp. 73-79.
10. H.A. Sawyer. Design of Concrete Frames for Two Failure Stages. In Flexural Mechanics of Reinforced Concrete, Proc., International Symposium, Miami, FL, 1964, ASCE, New York, Publ. 1965-50, 1965, pp. 405-437.
11. D.B. Beal. Destructive Testing of a Reinforced-Concrete T-Beam Bridge. Engineering Research and Development Bureau, New York State Department of Transportation, Albany, Res. Rept. 100, Dec. 1982.